Adjustable Three Color Optical Filters Using Ferroelectric - Dielectric Generalized Heterostructures Photonic Crystals

Behnam Kazempour[*,1], Fatemeh Moslemi[2]

[1] Department of physics, Ahar Branch, Islamic Azad University, Ahar, Iran

[2] Department of physics, Azarbaijan Shahid Madani University, Tabriz, Iran

Abstract: The current research is aimed to investigate the alterations of its optical features of novel adjustable three color narrowband optical filters, which comprise of blue, green and red light. A narrowband adjustable transmission optical filters according to dielectric- ferroelectric heterostructures photonic structures are designed using the transfer-matrix method (TMM). The dependence of the ferroelectric refractive index on the external applied voltage is considered in our investigations. The transmission spectra of the designed hetrostructures with the most valuable parameters, like repeat cycle counts number of PCs, external electric field, and incident angle for both TE and TM polarizations are numerically investigated. The results show that the transmission peaks of three color filter shift toward the shorter wavelength by increasing the incident angle for both polarization. Also, adjustability of the optical features of the proposed hetrostructures crystals external applied electric field is investigated .Therefore, these calculated results reveal an innovative idea for designing the tunable trichromatic filter and display applicationsthis.

Keywords: Photonic Crystal, External Voltage, Three-Color Filter, Band Gap.

1. INTRODUCTION

Photonic crystals (PCs) are   periodic   management of dielectric layers along some direction, with the distances between the adjacent units in order of a fraction of the optical wavelength [1-3]. In particular, PCs correspond to dielectric, metallic or semiconductor structures that present some kind of recurrence relation in their refractive indices [4-6]. By controlling and manipulating the flow of light in different frequency ranges and/or containing disparate PC structures with various widths, the reflectance, transmittance, and absorptance can be designed and modified. PCs can be the new raw material for making photonic circuits; this can be used as a filter optical diodes [7, 8], waveguides [9], sensors [10, 11], etc. For most recruitments, a defective PCs are

---

more favorable than the complete ones. Defect mode can be generated by interrupting the translation symmetry or structural periodicity of PC, and this defect state allows the transmission of light at a comparable frequency, and this advantage can be occupied in the model of optical filters [12-14] and multi-channel filters [15,16]. By modifying the number and thickness of defect layers, and use defined materials in photonic structure the multiple channeled optical filters can be produced to locate inside the photonic band gap (PBG) [17]. However, by increasing these parameters and use of the defined materials in photonic structures, the width of the PBG becomes narrow or compress, and the sidebands transmission cannot be restricted, this events confines the application of multichannel filters in PCs [18]. Several one-dimensional (1D) PCs with different optical properties are unified, photonic heterostructures can be created. Given that different PCs have various band gap widths, photonic heterostructures can display various characterizes [19]. Recently, much attention has been paid to vary the physical parameters of different hetrstructures PCs with a various layer thickness and materials that monochromatic transmittance of the multicolor filter can be achieved, so it has more superiority than the conventional dielectric PCs, which most of these structures are single- channel filters [20, 21]. Here, we scheme of color filters that is based of 1DPCs configurations by combining two PCs made up different kinds of materials containing adjustable refractive index and distinct thickness. The ingredients of the PC is composed of typical dielectric and ferroelectric layers in the presence of external electric field to create tunable trichromatic filters with non-transmission band gab in contrast to the transmission of conventional PCs. In fact, the advantage of placing ferroelectric in the considered structures to undertake this research resides in the fact that the authors have found no studies of heterostructures PCs with tunable optical filtering properties. It can be stated that the electro-optic photonic crystals have attracted much attention owing to their unique electromagnetic wave properties such as the ease of using the external electric field and the ability to control the physical parameters [22-24]. Our main goal is to study the possibility of constructing electro-tunable three-color filter in the visible region that is compound of two 1DPCs with three diverse materials and widths. The 1D dual-periodic PCs containing the ferroelectric layers with high transmission efficiency are characterized by a large non- transmission range and have three defects located in blue, green, and red light. Therefore, we apply the electro static bias perpendicular to our proposed structure. The influence of varying external voltage is illustrated that the position of the three channel filter red and blue shifted by applying the negative or positive biases, respectively. In additional, the possibility to achieve a tunable color filter is discussed through

changing the incident angle for both polarizations

2. THEORETICAL AND FORMULATION

Consider a 1DPC structure constituted by the periodic repetition of three different kinds of material layers in the presence of external electric field in the direction of propagation of light (z axis), as shown in Fig. 1. The proposed structure is composed of two different periodic PC units, $(AB)^q$ and $(CD)^q$, which q and p are the period number of (AB) and (CD), respectively. Here, A, D are assumed to be SiO_2 with refractive index $n_A = 1.5$ and B is considered MgF_2 with refractive index $n_B = 2.38$ [8, 22]. In this configuration C layers is assumed ferroelectric layer such as LiNbO3 (LNO) layer, when external voltage varies, it affects the index of refraction on C layer due to electro-optical effect. The photonic crystal unit cell constant is represented as a, d_A, d_B, d_C and d_D represent the thicknesses of A, B, C and D, respectively, and $d_A = 38\ nm$, $d_B = 63\ nm$, $d_C = 85\ nm$ and $d_D = 113\ nm$.
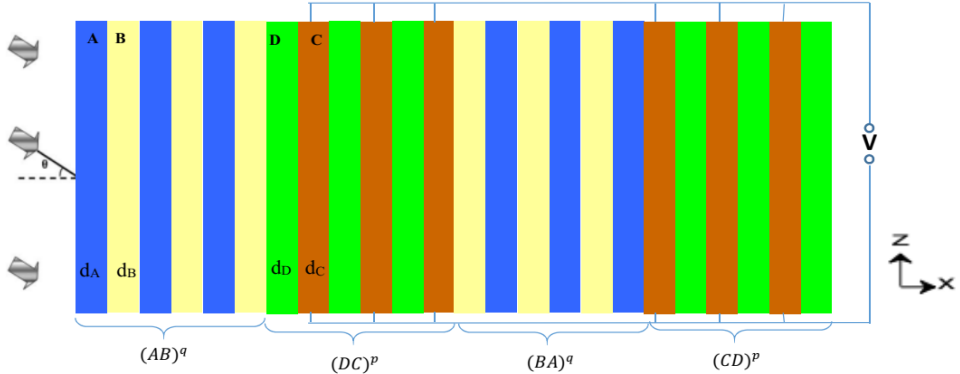
Fig. 1. Schematic drawing of $(AB)^q (DC)^p (BA)^q (CD)^p$. The external voltage is applied along the z direction.

The 4×4 transfer matrix method has been used to describe the optical properties of the multilayer structure composed of uniaxial and biaxial magneto-optic materials [23, 24]. In this work, it is used to investigate the transmission spectrum properties of the PC structure containing a uniaxial electro-optical

defect layer (LNO).Consider an electromagnetic wave with frequency of ω, electric and magnetic fields of E and H, respectively, incident to the structure with angle θ with respect to the z-axis. The fundamental equations for an electromagnetic wave are given by the following Maxwell equations:

$$
\vec{\nabla} \times \vec{E}(\vec{r},t) = i\omega\,\mu_0\,\vec{H}(\vec{r},t)
$$
$$
\vec{\nabla} \times \vec{H}(\vec{r},t) = -i\omega\,\varepsilon_0\,\vec{\varepsilon}\,\vec{E}(\vec{r},t)
$$
. \hfill (1)

After solving the Maxwell equations, it can be shown that the equation governing the tangential components of the electric and magnetic fields is [23]:

$$
\frac{\partial \psi}{\partial z} = ik_0 \Delta \psi ,
\tag{2}
$$

where $k_0 = \omega/c$ is the vacuum wave vector, ψ is vector $\left(\sqrt{\varepsilon_0}E_x, \sqrt{\mu_0}H_y, \sqrt{\varepsilon_0}E_y, \sqrt{\mu_0}H_x\right)$, and Δ is a coefficient matrix with elements that depend on the optical properties of the medium . LNO is an anisotropic electro-optic uniaxial crystal with a relative permittivity tensor of [25- 27]:

$$
\varepsilon = \begin{pmatrix} \varepsilon_x & 0 & 0 \\ 0 & \varepsilon_y & 0 \\ 0 & 0 & \varepsilon_z \end{pmatrix} = \varepsilon_0 \begin{pmatrix} n_o^2 & 0 & 0 \\ 0 & n_o^2 & 0 \\ 0 & 0 & n_e^2 \end{pmatrix}.
\tag{3}
$$

When the external electric field is applied parallel to the optical axis of the crystal and the optical axis falls along the z-axis (Fig. 1), the ordinary and extraordinary refractive indices are given as [30]

$$
n_e(V) = n_e(\theta) - \frac{1}{2} n_e(\theta)^3 r_{33} \left(\frac{V}{D}\right)
\tag{4}
$$

$$
n_o(V) = n_o - \frac{1}{2} n_o^3 r_{13} \left(\frac{V}{D}\right),
\tag{5}
$$

where r_{33} and r_{13} are the electro-optical coefficients, and $D = 0.5mm$ is the distance between the two electrodes in the direction of Z-axis. and $n_e(\theta)$ is the extra-ordinary refractive index which is dependent on the incident angle as,

$$\frac{1}{n_e(\theta)^2} = \frac{\cos\theta^2}{n_e^{\ 2}} + \frac{\sin\theta^2}{n_o^{\ 2}}, \tag{6}$$

here, n_e and n_o are the extra-ordinary and the ordinary refractive indexes parallel and perpendicular of the optical axis, respectively. Solving Eq. (2) for LNO layer, where the principal axes coincide with the x, y and z axes, the coefficient matrix Δ is given as

$$\Delta_{LNO} = \begin{pmatrix} 0 & 1-N_x^2/\varepsilon_z & 0 & 0 \\ \varepsilon_x & 0 & 0 & 0 \\ 0 & 0 & 0 & 1 \\ 0 & 0 & \varepsilon_y - N_x^2 & 0 \end{pmatrix}, \tag{7}$$

here, $N_x = n_0\sin\theta$, where n_0 and θ are the refractive index of the incident medium and incident angle, respectively. It has been shown that the elements of the transfer matrix depend on the eigenvalues of matrix Δ. After algebraic calculation, the eigenvalues of Δ_{LNO} matrix can be defined as:

$$\alpha_{1z} = \sqrt{\varepsilon_x(1-N_x^2/\varepsilon_z)}, \alpha_{2z} = \sqrt{\varepsilon_y - N_x^2}. \tag{8}$$

The eigenvectors corresponding to the eigenvalues α_{iz} are the elements of Δ_{LNO} matrix. Solving Eq. (2) using the eigenvalues and eigenvectors of matrix Δ_{LNO} shows that the tangential components of the fields through the LNO layer can be transferred as follows:

$$\psi(z+d_4) = M_{LNO}(d_4)\psi(z), \tag{9}$$

where M_{LNO} is the 4×4 transfer matrix of the anisotropic LNO layer and is given by

$$M_{LNO} = \begin{pmatrix} \cos(k_0\alpha_{1z}d_4) & \dfrac{ik_{z1}\sin(k_0\alpha_{1z}d_4)}{\Delta_{12}} & 0 & 0 \\ \dfrac{i\Delta_{12}\sin(k_0\alpha_{1z}d_4)}{\alpha_{1z}} & \cos(k_0\alpha_{1z}d_4) & 0 & 0 \\ 0 & 0 & \cos(k_0\alpha_{2z}d_4) & \dfrac{i\sin(k_0\alpha_{2z}d_4)}{\alpha_{1z}} \\ 0 & 0 & ik_{z1}\sin(k_0\alpha_{2z}d_4) & \cos(k_0\alpha_{2z}d_4) \end{pmatrix}. \tag{10}$$

The dielectric permittivity tensors for the A, B, and D layers, which are isotropic, are given as

$$\varepsilon = \begin{pmatrix} \varepsilon_j & 0 & 0 \\ 0 & \varepsilon_j & 0 \\ 0 & 0 & \varepsilon_j \end{pmatrix} (j = A, B, D)^{\cdot} \tag{11}$$

Also, the coefficient matrix Δ and the transfer matrix M for A, B and D layers can be calculated by the same method as follows

$$\Delta_j = \begin{pmatrix} 0 & 1 - N_x^2/\varepsilon_j & 0 & 0 \\ \varepsilon_j & 0 & 0 & 0 \\ 0 & 0 & 0 & 1 \\ 0 & 0 & \varepsilon_j - N_x^2 & 0 \end{pmatrix}, \tag{12}$$

$$M_j = \begin{pmatrix} \cos(k_0\alpha_{jz}d_j) & \dfrac{i\alpha_{jz}\sin(k_0\alpha_{jz}d_j)}{\varepsilon_j} & 0 & 0 \\ \dfrac{i\varepsilon_j\sin(k_0\alpha_{jz}d_j)}{\alpha_{jz}} & \cos(k_0\alpha_{jz}d_j) & 0 & 0 \\ 0 & 0 & \cos(k_0\alpha_{jz}d_j) & \dfrac{i\sin(k_0\alpha_{jz}d_j)}{\alpha_{jz}} \\ 0 & 0 & i\alpha_{jz}\sin(k_0\alpha_{jz}d_j) & \cos(k_0\alpha_{jz}d_j) \end{pmatrix}, \tag{13}$$

here $\alpha_{jz} = \sqrt{\varepsilon_j - N_x^2}$ and d_j is the thickness of the corresponding layer. The total transfer matrix representing the entire structure is given as

$$\begin{aligned} M &= (M_A M_B)^5 M_{Ag} M_{LNO} M_{Ag} (M_B M_A)^5 \\ &= \begin{pmatrix} M_{11} & M_{12} & M_{13} & M_{14} \\ M_{21} & M_{22} & M_{23} & M_{24} \\ M_{31} & M_{32} & M_{33} & M_{34} \\ M_{41} & M_{42} & M_{43} & M_{44} \end{pmatrix} \end{aligned}^{\cdot} \tag{14}$$

After a series of algebraic calculations applying the boundary conditions to the interfaces of the layers, the relation between the incident, reflection, and transmission fields can be expressed as [23,24]:

$$\begin{pmatrix} E_{TM}^i \\ E_{TM}^r \\ E_{TE}^i \\ E_{TE}^r \end{pmatrix} = \begin{pmatrix} M_{11} & M_{12} & M_{13} & M_{14} \\ M_{21} & M_{22} & M_{23} & M_{24} \\ M_{31} & M_{32} & M_{33} & M_{34} \\ M_{41} & M_{42} & M_{43} & M_{44} \end{pmatrix} \begin{pmatrix} E_{TM}^t \\ 0 \\ E_{TE}^t \\ 0 \end{pmatrix}, \tag{15}$$

where E_{TM}^i, E_{TM}^r, E_{TE}^i, E_{TE}^r, E_{TM}^t and E_{TE}^t denote the complex amplitudes of the TE and TM modes of the incident, reflected, and transmitted waves, respectively. For example, the transmission coefficients of the TM- and TE-polarized waves are,

$$t_{TM} = \left(\frac{E_{TM}^t}{E_{TM}^i}\right)_{E_{TE}^i = 0} = \frac{M_{33}}{M_{11}M_{33} - M_{13}M_{31}} .$$

$$t_{TE} = \left(\frac{E_{TE}^t}{E_{TE}^i}\right)_{E_{TM}^i = 0} = \frac{M_{11}}{M_{11}M_{33} - M_{13}M_{31}}$$

(16)

The corresponding transmittances are $T_{TM} = |t_{TM}|^2$ and $T_{TE} = |t_{TE}|^2$.

## 3. Results and Discussion

From Eq. (3) it can be observed that the refractive index is linearly proportional to the applied external voltage, so that positive voltages are reducing the index of refraction and negative biases are increasing it. It is worth stressing that the voltage breakdown of LNO exceeds 10^7 V/cm [28-30]. Both substrates surrounding the PC are simply assumed to be air. First, we concentrate on finding the optimal number of periods (q and p) that utilize PBG and design optical filter without introducing defect layers. The numerical calculations are performed for the $V = 0$ and $\theta = 0^\circ$. Fig. 2 shows Figures 2(a) and 2(b) present the calculated transmittance spectra of two PCs composed solely of units $(AB)^9$ and $(DC)^9$, respectively. These spectra exhibit two different PBGs because of their difference in lattice constants. It is seen that in Fig. 2(b), the bandgap of the structure shifts to the longer wavelength, and its bandwidth broadens as the lattice constant increases. Figure 2(c) shows the transmittance spectra of the 1D dual-periodic structure $(AB)^9(DC)^9$ composed of two different of 1D PCs. The PBG of $(AB)^9(DC)^9$ overlaps the bandgaps of $(AB)^9$ and $(DC)^9$ because $(AB)^9(DC)^9$ is composed of $(AB)^9$ and $(DC)^9$. Also, the band gap of this configuration overlaps the total visible wavelengths utilized as an optical reflector.
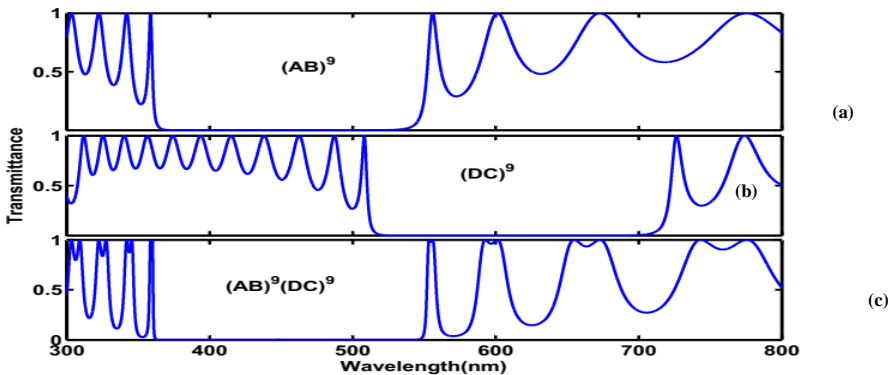
Fig. 2. Transmittance spectrum of 1D PCs $(AB)^9$, $(DC)^9$, and $(AB)^9(DC)^9$, the relationship between 1D PCs. (a) $(AB)^9$.(b) $(DC)^9$. (c) $(AB)^9(DC)^9$.

Owing to the creating of the widened PBG of the above PC structure $(AB)^9(DC)^9$ to changing arrangement of structures by combine to form with dual-periodic PC structure, $(AB)^4(BA)^4(DC)^4(CD)^4$. By changing the units of proposed structure are considered as defect layers because the disorder is introduced into the periodic structures. Figures 3 show the transmittance spectra of 1DPC structures $(AB)^4(BA)^4(DC)^4(CD)^4$. It is shown that in the proposed hetrostructure, light penetrates the PCs through resonating tunneling and can obtain more tunneling peaks, called defect modes. Therefore, three defect modes located at 447.5, 521.2 and 605.4 nm, respectively, are observed (Fig. 3). These defect modes sets to blue, green and red light, respectively. This feature of the photonic heterostructure offers a probable way for the design of various color defect modes in the visible range. This behavior also acts convenience for the design of color filters with various defect modes with high transmittance.
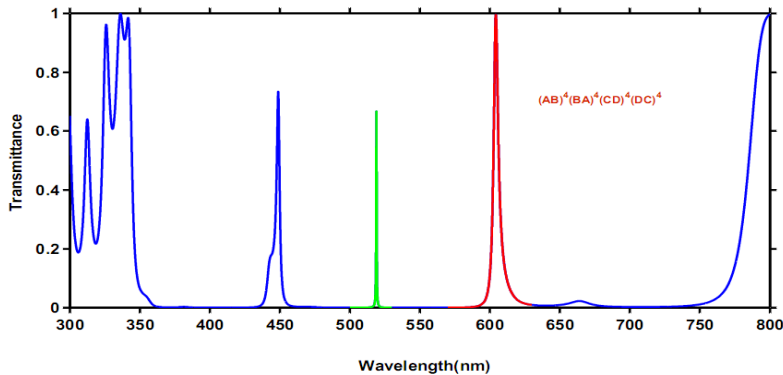

Fig.3. Transmission spectra of $(AB)^4(BA)^4(DC)^4(CD)^4$ when p and q has same values.

Considering the various factors that affect the position, number and transmittance of filters, the search areas for the number of periods of the heterostructures and external applied voltage have to be determined. In this section, we analyze the repeat cycle counts q and p parameters of the photonic heterostructures on the transmittance spectra. We can see from Fig. 4 that, by changing the repeat cycle counts structure, to achieve defect modes with high transmittance in the blue, green and red light

over the entire visible region, is considered as the final outcome. A superior result can be obtained when q and p is equal to 5 and the ideal condition is obtained when q is equal to 5 , as shown in Fig.4(a). Also, notice that the intensity transmissions of the defect modes by choosing $q = 6$ in the Fig.4 (b), which can lead to the enhanced transmission of the proposed structure compared with the case $q = 5$.
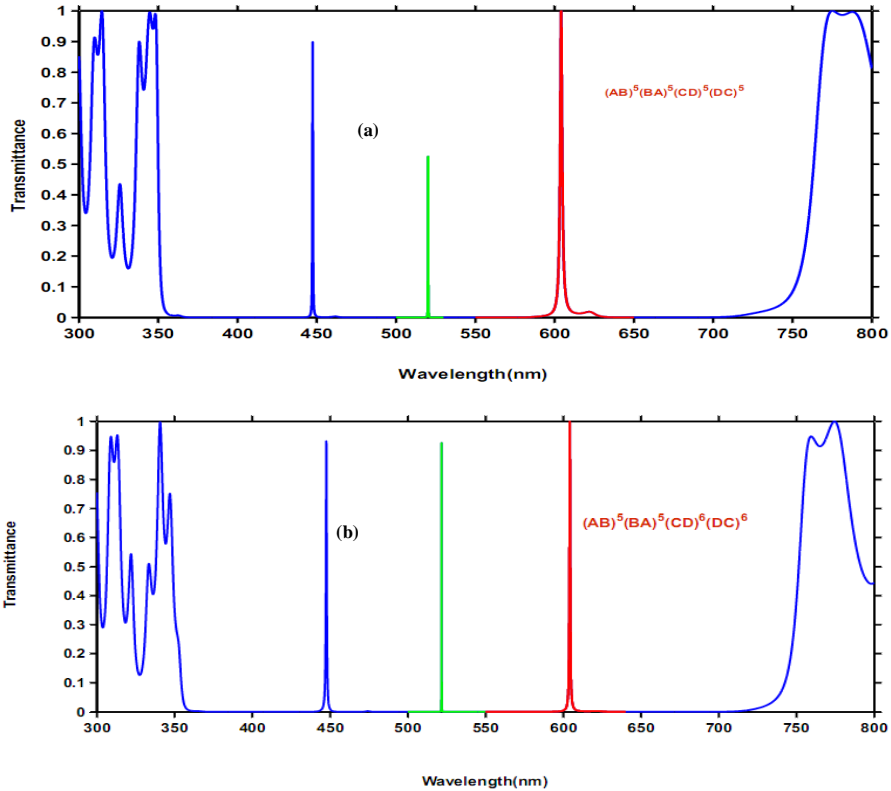
Fig. 4. Relationship between different 1DPCs heterostructures and the intensity transmission of the defect modes.

In the next stage, the influence of the external applied voltage on the transmission behavior for optimized structure as mentioned with configuration $(AB)^5(BA)^5(DC)^6(CD)^6$, has been investigated as a possibility for flexible control of the transmission peak. With regards to Eq. (3), the effective refractive index of the LNO increases with increase in the applied negative voltage, while, it decreases with increase in the applied positive voltage. Figure 5 (a) displays

transmission spectra as a function of the light wavelength for different applied external voltages, at normal incidence angle ($\theta = 0^\circ$). It is important to note that, we just consider the wavelength regions around the defect positions. As it can be seen from this figures that, there are nearly perfect transmissions (modes 2 and 3) for all values of the applied voltages and the peak wavelength of the defect modes moves toward shorter wavelengths (blue shift) by increasing the applied external voltage from 0 kV to 400 kV, at modes 2 and 3. Also, It can be seen from Fig.5 (b), that the defect modes (modes 2and 3) are red shifted for negative biases voltage. This shifting property indicates that the structure can be utilized to design a tunable optical filter. Furthermore, it can be understood from this figure that the transmission peak of mode (1) remain almost constant by increasing for both biases voltage.
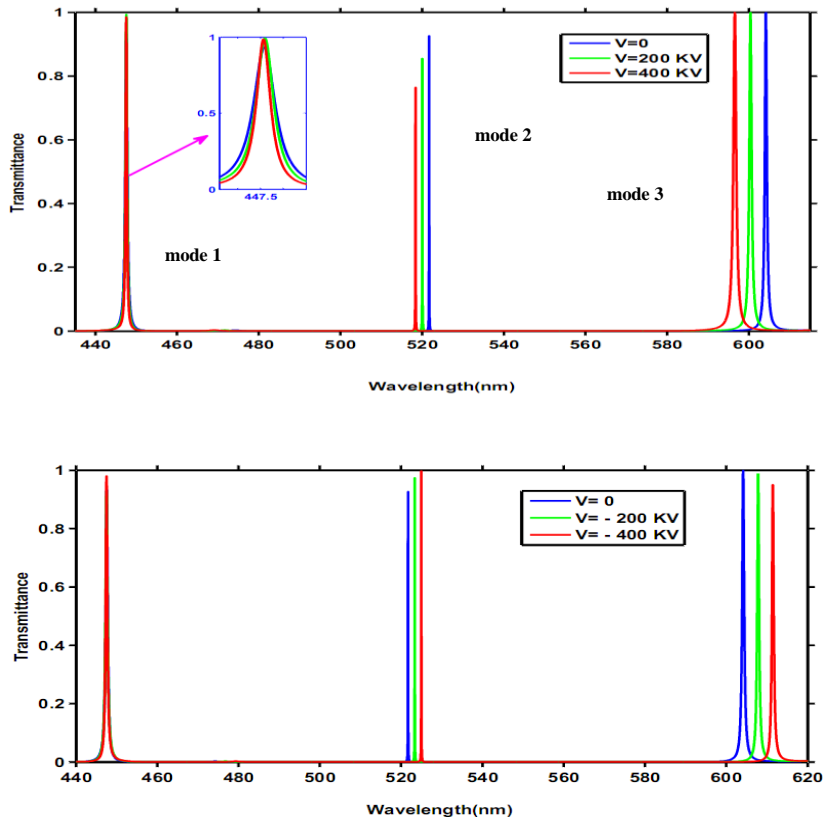
Fig. 5. Transmission as a function of wavelength of designed structures at positive biases (a) and negative biases (b) with different applied voltages, at normal incidence angle ($\theta = 0^\circ$).

The optical properties of conventional filters are relevant to the incidence angle and polarization of the incident light for both the positive and negative voltage. The results are shown in Fig. 6, at fixed applied voltage of $\pm 200 \ KV$ and $\pm 400 \ KV$. It can be seen that in the both polarizations the defect mode shifts toward the lower wavelengths as the incident angle increases for both the positive and negative biases. Also, the peak height of optical filters for TE waves decreases as the angle of incidence increases. In additional, it can be seen that the defect modes are compressed and broadened with increasing of the angle, for TM and TE polarization, respectively. So, we can deduce the TE-polarized waves more sensitive to the angle change than TM-polarized waves.
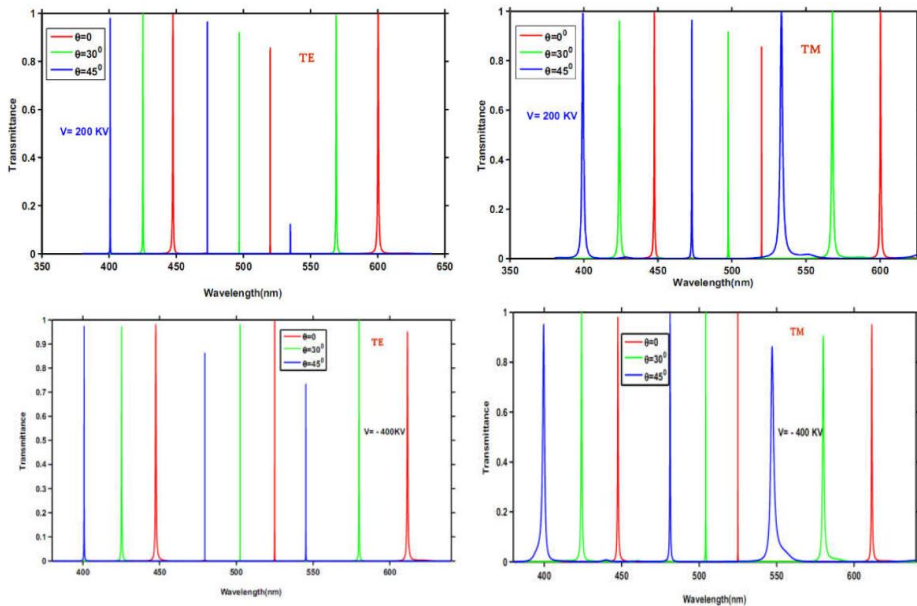
Fig. 6. Transmittance spectrum of proposed 1DDPC structure at different incident angles for TE and TM polarizations in two externally applied voltages of 200 KV and - 400KV.

For more clarity, the behaviour of peak wavelength of the three colour filter and PBG on the variation of the incidence angle is illustrated in Fig.7 for both polarization, at a specified value of the external voltage (V=200KV). An

incidence angle dependent defect modes and PBG is clearly seen. It is apparent that the defect modes are blue shifted as the incidence angle increases for both TE and TM polarization. Also, the width of the PBG are decreased as the angle of incidence increases. In the TM polarized wave, the PBG is narrowed when the angle increases. Whilst, in the TE polarized wave, the PBG is broadened by increasing the incident angle. This feature is sharply contrasted to the case of using the usual structure. These results indicates the design three color optical filter with an external adjustable factor that can be more useful to design modern optical devices.
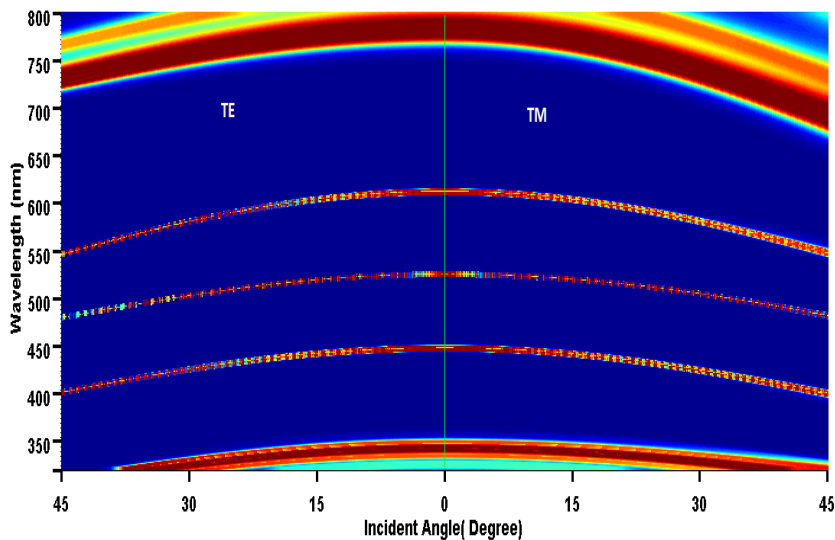
Fig.7. Dependence of defect mode peak wavelength on incident angle for TE and TE polarizations at fixed external voltage of 200 KV.

4. CONCLUSIONS

In conclusion, the transmission properties of 1DPCs aperiodic dual heterostructures have been investigated theoretically and numerically. the possibility integrate of the photonic structures permits to build a new class of heterostructures photonic crystals which exhibit an original characteristics and design tunable three color filters and narrowband filters for ordinary improved structure in terms number of period's structures, external applied voltage, and incidence angle for TE and TM mode in the visible region is investigated. The numerical results indicate that, by applying an external positive bias of 0–400 kV in the x-direction to the

ferroelectric layers, the wavelength positions of the optical filters in the transmission spectra blue shift. But a red shift is observed in negative biases. Also, the peak wavelength of the defect modes have a blue shift as the increase the angle of incidence for both TE and TM waves. In additional, for TE polarization, the width of the PBG is broadened and vice-versa for TM polarization. This heterostructure can be applicable for the designing of tunable three-color filters for various optoelectronics applications of potential interest in the fields of photonics and optoelectronics in the visible region.

Reference

[1] K. Sakoda, Optical Properties of Photonic Crystals, Springer-Verlag, Berlin (2001)).

[2] J. D. Joannopoulos, R. D. Meade, J. N.Winn, Photonic Crystals: Molding the Flow of Light,   Princeton University Press, Princeton, NJ (1995).

[3] M. Skorobogatiy, J. Yang, Fundamentals of Photonic Crystal guiding, Cambridge University   Press (2009).

[4] B. Xu, G. Zheng, Y. Wu, Narrow band and angle insensitive filter based on one dimensional photonic crystal containing graded index defect, Mod. Phys. Lett.B. **29**, 128-136 (2015).

[5] A. H .Aly, S.A. El-Naggar, H.A.Elsayed, Tunability of two dimensional n-doped semiconductor photonic crystals based on the Faraday effect, Optics Express **23**, 15038-15046 (2015).

[6] A. Gharaati, H. Azarshab, Characterization of defect modes in one-dimensional ternary metallo-dielectric nanolayered photonic crystal, PIER B **37**, 125-141 (2012).

[7] B. Kazempour, K. J-Ghaleamshidih, Use of uniaxial ferroelectric material as a tunable double-optical filter based on polarization converter and splitting in photonic crystal, Optik **168** , 839-846 (2018).

[8] K. Jamshidi- ghaleh and B. Kazempour, Effect of incident angle and polarization on electrically-tunable defect mode in anisotropic photonic crystal, Appl. Opt. **55**, 4350-4357 (2016).

[9] N. Taleb, Optical modes in slab waveguides with magneto electric effect, J. Opt. **18**, 055607 (2016).

[10] Z. Baraket, J. Zaghdoudi, M. Kanzari , Investigation of the 1D symmetrical linear graded superconductordielectric photonic crystals and its potential

applications as an optimized low temperature sensors, Optical Materials **64**, 147-151 (2017).

[11] S. A. Shaheen, and S. A. Taya, Propagation of p-polarized light in photonic crystal for sensor application, Chinese Journal of Physics. **55**, 571-582 (2017).

[12] C.-J. Wu, Z.H. Wang, Properties of defect modes in one dimensional photonic crystals. Prog. electromagn. Res. **103**, 169–184 (2010).

[13] K. Jamshidi- Ghaleh, B. Kazemour, and A. Phirouznia, Electrically Tunable Polarization Splitting and Conversion Based on 1DPC Structure with Anisotropic Defect Layer, Superlattices and Microstructures **101**, 109-116 (2017).

[14] S. Roshan Entezar, Z. Saleki, A. Madani, Optical properties of a defective one-dimensional photonic crystal containing graphene nanaolayers, Physica B **478**, 122-126 (2015).

[15] S. Kumar Awasthi, R. Panda, and L. Shiveshwari, Multichannel tunable filter properties of 1D magnetized ternary plasma photonic crystal in the presence of evanescent wave, Phys. Plasmas **24**, 072111 (2017) .

[16] P. N .Li, Y .W.Liu, Multichannel filtering properties of photonic crystals consisting of single-negative materials, Phys. Lett. A **373**, 1870-1873 (2009).

[17] A. H. Aly , H. A. Elsayed, Defect mode properties in a one-dimensional photonic crystal, Physica B **407**, 120–125 (2012).

[18] M. J. P. Loschialpo, and J. Schelleng, Photonic band gap structure and transmissivity of frequency-   dependant metallic-dielectric systems, J. Appl. Phys. **88**, 5785-5790 (2000).

[19] Z.S. Wang, L. Wang, Y.G. Wu, L.Y. Chen, X.S. Chen, W. Lu, Multiple channeled phenomena in heterostructures with defects mode , App. Phys. Lett. **84**, 1629 (2004).

[20] G. Q. Liang, P. Han, and H. Z. Wang, Narrow frequency and sharp angular defect mode in one-dimensional photonic crystals from a photonic heterostructure, Opt. Lett. **29**, 192–194 (2004).

[21] L. Wang, Z.S. Wang, Y.G. Wu, L.Y. Chen, S.W. Wang, X.S. Chen, W. Lu, Enlargement of the nontransmission frequency range of multiple-channeled filters by the use of heterostructures, J. App. Phys. **95**, 424 (2004).

[22] K. J. Ghaleh and B. Kazempour, External tunability of optical filter in symmetric one-dimensional photonic crystals containing ferroelectric and ITO material defect, Optik **127** , 10626–10631 (2016).

[23] I. Abdulhalim, Analytic propagation matrix method for linear optics of arbitrary biaxial layered media, J. Opt. A **1**, 646 (1999).

[24] P. Yeh, Electromagnetic propagation in birefringent layered media, J. Opt. Soc. Am. **69**, 742 (1979).

[25] A. Yariv and P. Yeh, Optical Waves in crystals propagation and control of laser radiation, Wiley and Sons, New York (1983).

[26] B.E. Saleh, M.C. Teich, B.E. Saleh, Fundamentals of Photonics, vol. 22, Wiley, New York (1991).

[27] M. Born and E. Wolf, Principles of Optics, 7th (expanded) ed. Cambridge University (1999).

[28] A. Rashidi, A. Namdar a, R.A. Ghaleh, Absorption behavior in graphene-based one-dimensional photonic crystals containing a x-cut lithium niobate layer, Sup. Micro. **105**, 74-80 (2017).

[29] G. Rosenman, P. Urenski, A. Agronin and Y. Rosenwaks, Submicron ferroelectric domain structures tailored by high-voltage scanning probe microscopy, Appl. Phys. Lett. **82**, 103 (2003).

[30] M. Molotskii, A. Agronin, P. Urenski, M. Shvebelman, G. Rosenman, Y. Rosenwaks, Ferroelectric domain breakdown, Phys. Rev. Lett. **90** (10), 107601-10760 (2003).